

Ferroelasticity of t' -Zirconia: I, High-Voltage Electron Microscopy Studies of the Microstructure in Polydomain Tetragonal Zirconia

 Dietmar Baither,[†] Bernd Baufeld,[‡] and Ulrich Messerschmidt[§]

Max Planck Institute of Microstructure Physics, Halle (Saale), D-06120, Germany

Andreas H. Foitzik and Manfred Rühle*

Max Planck Institute of Metals Research, Stuttgart, D-70174, Germany

The microstructure of polydomain tetragonal zirconia (t' -ZrO₂), i.e., a ZrO₂ modification exhibiting ferroelastic behavior, is studied by high-voltage electron microscopy. This material consists of three domain variants of the tetragonal phase with their c -axes nearly orthogonal to each other. Always two variants of these platelike domains are alternately arranged, forming elongated regular colonies. Hence, in both variants the common habit plane of the domains is a {110} twin plane. The colonies are of columnar shape with a <111> longitudinal axis. They are bound by {110} planes, too, which are twin planes for the domains in the contiguous colonies. Owing to their particular structure and the helical arrangement of the adjoining colonies, the material remains coherent and pseudocubic over large macroscopic regions, although it is formed by different tetragonal domains.

I. Introduction

IN MANY zirconia-based ceramic materials, transformation toughening is the dominant toughening mechanism, based on the martensitic transformation of the tetragonal phase into the monoclinic one. High strength and fracture toughness of tetragonal polydomain zirconia (t' -zirconia) with an yttria content of 3 mol%, however, are attained by a ferroelastic transformation.¹ At 1100°C the strength is twice as high as in fully stabilized (cubic) zirconia, although this temperature is well above the equilibrium transition temperature between the tetragonal and monoclinic phases. Accordingly, no monoclinic phases had been found in the stressed samples.^{2,3}

The ferroelastic transformation process differs from the stress-induced martensitic transformation in the fact that there is no change in the crystal structure, but a reorientation of the ferroelastic domains. Ferroelastic properties of tetragonal zirconia arise from a symmetry-lowering ferroic phase transition of the cubic parent phase, resulting in three energetically equivalent orientation states, also called twin variants or domains. These domains, mutually in nearly orthogonal arrangement, form pseudocubic crystals. Under stress, domains can reorient their c -axes to accommodate the strain.⁴ The details of this

effect were investigated by several authors.¹⁻⁶ They depend on the direction and sign of the stress with respect to the crystal orientation and equal domain switching in ferroelectric and ferromagnetic materials. Uniaxial compression tests on t' -zirconia revealed the stress-strain hysteresis, a characteristic feature of ferroelastic materials.⁷ Moreover, the stress-strain behavior was measured as a function of strain rate and temperature.⁸

As one component of the microstructure of this material, the nature of the domain walls was analyzed by high-resolution electron microscopy.⁹ The individual domains form colonies which themselves are frequently arranged in very regular structures, sometimes described as "herringbone" domain structures.³ As in t' -zirconia, the tetragonal domains fill the whole volume, their spatial arrangement has to be highly symmetrical in order to minimize the coherency strain energy. It may therefore be expected that the three-dimensional arrangement of the colonies differs from that in partially stabilized zirconia, in which the colonies of tetragonal domains are embedded in a uniform matrix (e.g., Ref. 10). There is almost no information available on this regular arrangement of the colonies in t' -zirconia. It can be gained by applying high-voltage electron microscopy (HVEM) to relatively thick specimens, facilitating the reconstruction of the real three-dimensional structure. This is the subject of Part I of the present paper. Similarly, the microprocess of domain switching has never been observed directly. High-temperature *in situ* straining experiments were therefore performed inside the HVEM. They are described in Part II.

II. Experimental Procedure

ZrO₂ single crystals of 3 mol% Y₂O₃ (Ceres, North Billerica, MA) were prepared by the skull melting technique. From these crystals, 2 × 2 × 8 mm³ specimens were cut in the shape of parallelepipeds with faces orthogonal to the <100> pseudocubic axes. The t' -phase was obtained by heating the samples within the cubic phase field at 2150°C for 10 min. Subsequently, the samples were furnace-cooled to room temperature within 60 min to prevent crack nucleation. In this temperature range, diffusion effects are negligible, owing to the sluggish cation diffusion. TEM samples for structure investigations were prepared by standard methods, dimpling and ion milling down to a final thickness of about 0.5 μm. The microscope used for diffraction contrast experiments was a JEOL HVEM, operating at an accelerating voltage of 1000 kV and equipped with a 45° double-tilting goniometer stage.

III. Results and Discussion

It is well known that in tetragonal zirconia three variants of tetragonal domains occur with their c -axes nearly parallel to the cube axes of the parent phase. They are denoted by t_1 , t_2 , and t_3 according to their respective c -axes being parallel to the [100],

David R. Clarke—contributing editor

Manuscript No. 191586. Received August 19, 1996; approved April 5, 1997.

Presented at a Symposium on Microstructure-Property Relations of Advanced Materials, a symposium in honor of Professor Arthur Heuer's 60th birthday, held at Max-Planck-Institut für Metallforschung, Stuttgart, Germany, April 29–30, 1996.

Supported by the Deutsche Forschungsgemeinschaft (DFG).

*Member, American Ceramic Society.

[†]Present address: Max Planck Institute of Metals Research, Stuttgart D-70174, Germany.

[‡]Present address: Japan Science and Technology Corporation (JST), Nagoya, 456, Japan.

[§]Author to whom correspondence is to be addressed.

[010], and [001] axes of the cubic parent. These domains form ordered colonies with two alternating variants always sharing the same {110} habit plane, which is a twin plane for both variants.¹¹ In t' material, the colonies fill the whole volume, thus directly adjoining each other and mostly exhibiting a regular outer shape, which has not been analyzed previously.

In the (100)-oriented foils, which are usually investigated, two structures are typical, as demonstrated in Fig. 1.

(a) Colonies of domains with domain boundaries differently inclined with respect to the surface adjoining parallel to a $[01\bar{1}]$ plane, which is perpendicular to the foil surface. These colonies appear elongated in the $[011]$ direction.

(b) Colonies with inclined domain boundaries adjoin colonies with perpendicularly arranged domain boundaries. The interface between both colonies is again of the {110} type, but the $(10\bar{1})$ plane is now inclined to the surface and the colonies exhibit a $[010]$ longitudinal axis.

The arrangement of the platelike domains in the different colony structures is schematically drawn in Figs. 2(a) and (b). According to the cube symmetry, two configurations of the above structures may occur, rotated by 90° . It is a striking feature that two colonies always share one set of domains, e.g., t_1 in Fig. 2(a) or t_2 in Fig. 2(b). This is visible only under specific contrast conditions as in Fig. 3.

In spite of the relatively thick specimens used for HVEM, both structures represent only thin sections through the real three-dimensional arrangement of the colonies. This and the contrast superposition inhibit recognition of the third habit plane of the colonies, thus requiring various considerations for the complete three-dimensional reconstruction. It is proposed in the present paper that all colonies are of the same kind; i.e., they are entirely bound by {110} faces and elongated in $\langle 111 \rangle$ directions, which are the intersection lines between the colony boundaries. Hence, all three outer faces of the colonies make angles of 60° . Always one set of domains penetrates through the colony boundaries, while the other two sets meet at the colony boundaries, with the boundary plane being a twin plane of the adjoining variants. Figure 4 schematically shows this morphology for the three "inclination variants" of the platelike domains with respect to the longitudinal axis of the colony.

The suggestion that the different appearance of the colony structure in different sections originates from a single microstructure can be verified as follows. For the sake of convenience, the colonies in structure (a) are denoted by $C_1 = t_1/t_2$ and $C_2 = t_1/t_3$, and in structure (b) by C_1 and $C_3 = t_2/t_3$, where t_1 , t_2 , and t_3 correspond to the three domain variants mentioned above. In lateral view ([001] direction in Fig. 2(a)) of the colony structure (a) with all domain boundaries inclined to the (100) surface, the domain boundaries of colony C_1 appear in edge-on orientation. The lateral $(01\bar{1})$ boundary of the colony would then be inclined to the hypothetical (001) surface by 45° . Since in the micrographs solely one type of colony occurs with its domains in edge-on orientation, one can conclude that these colonies (C_3) have the same orientation with respect to the (100) plane as those with inclined domains (C_1) in relation to the (001) plane, because all cube directions are equivalent. A similar consideration also applies to the lateral viewing direction of the colonies (C_3) containing domains in edge-on orientation. Then, all habit planes of the colonies and domains, respectively, are known, resulting in a $\langle 111 \rangle$ longitudinal axis of the colonies, as shown in Fig. 4. In the micrographs, the distinct images of the colony structure arise from thin sections through the colonies, formed by domains with boundaries differently inclined with respect to the longitudinal axis of the colony (cf. Fig. 4).

Colonies with parallel longitudinal axes may repeatedly be joined. The domains either extend through both neighboring colonies or they meet at the colony border in a twin plane, with the same twinning relations as between the domains within the colonies. Thus, accordionlike structures may be formed with both lateral dimensions of the colonies varying considerably.

The question arises whether three colonies may also be linked along their $\langle 111 \rangle$ edges in such a way that the volume is completely filled. Within the framework of the previous approach this is geometrically possible as shown schematically in Fig. 5. Figures 5(a) and (b) demonstrate two layers out of a threefold arrangement of colonies in a $[111]$ projection parallel to the longitudinal axes of the colonies. The layers in Figs. 5(a) and (b) have to be stacked alternately on each other to form the whole arrangement of the three colonies. If these three colonies meet exactly along their $[111]$ edge as in Figs. 5(a)

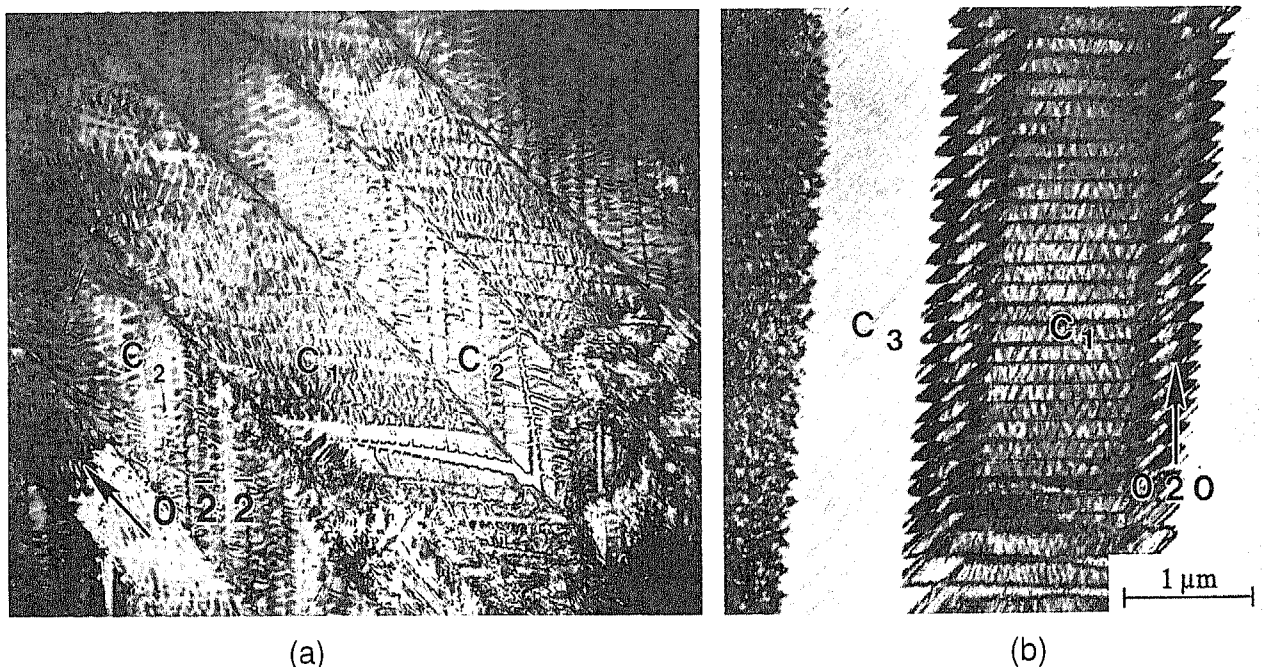


Fig. 1. Tetragonal domains forming colonies. The arrows in the figures show the imaging diffraction vectors. Close to the $[100]$ pole. (a) Colonies C_1 and C_2 of domains with boundaries differently inclined to the foil plane adjoin on $(01\bar{1})$ planes, which are perpendicular to the foil surface. (b) Colonies C_1 of domains with boundaries inclined to the surface and colonies C_3 of domains in perpendicular arrangement to the surface adjoin on $(10\bar{1})$ planes, which are inclined.

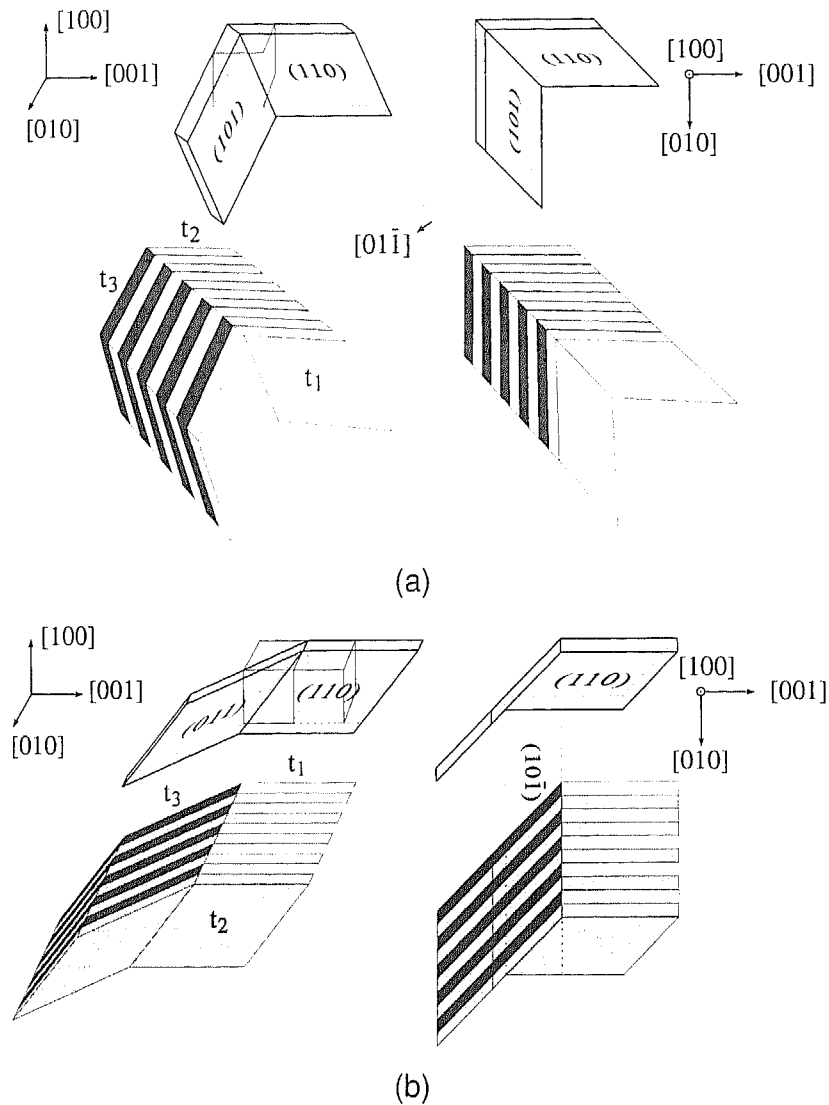


Fig. 2. Schematic view of the colony structures imaged in Figs. 1(a) and (b), in perspective (left) and in projection in $[100]$ direction (right). The drawings in Fig. 2(a) refer to Fig. 1(a), and in Fig. 2(b) to Fig. 1(b), respectively.

and (b), then one colony boundary is not a twin plane of the adjoining domains. In the example chosen in the figure, the $(1\bar{0}1)$ colony boundary of the first layer (Fig. 5(a)) is a twin plane for the t_1 and t_3 domains but the $(\bar{1}10)$ colony boundary is not. The same holds for the second layer (Fig. 5(b)) with the variants t_3 and t_2 . Again, the $(\bar{1}10)$ colony boundary is not a twin plane. Similar situations exist for the other possible combinations of the three variants. Moreover, at those colony boundaries which are not twin planes of the adjoining domains, different domain variants would always meet in all layers. This, as well as disturbed twin relations, was never observed. As discussed above (Fig. 3), always one domain variant extends into the neighboring colony, and in the subsequent layer such domain variants adjoin, for which the colony boundary is a twin plane. Thus, it may be concluded that the colonies have to be linked in another way to form the threefold arrangement.

A solution is given if the three colonies do not exactly adjoin along their $\langle 111 \rangle$ longitudinal edges, but only outside a "core region," as indicated in Figs. 5(c) and (d). Due to the funnel-like inclination of the three domains, a shift of the colonies C_1 and C_3 with respect to C_2 out of the core region, as indicated by the arrows, is connected with an upward shift of the domain t_3 of colony C_3 . If this upward shift equals the domain distance in the $[111]$ direction, the domain t_3 in C_3 of the lower layer (Fig. 5(c)) meets t_3 of C_2 of the upper layer (Fig. 5(d)), resulting in a helical structure around the $[111]$ longitudinal axis. In the

next turn, t_2 of C_3 meets t_1 of C_2 . This time, the $(\bar{1}10)$ colony boundary is the correct twin plane. The screwlike or helical structure formed was schematically shown already in Fig. 4. Small strains remain at the boundaries, which will be discussed later. According to the proposed model, all interfaces, i.e., the domain and the colony boundaries, are twin planes. Thus, the colony boundaries are smooth in contrast to their faceted morphology in partially stabilized zirconia.¹⁰

The superposition of the strong domain contrasts prevents direct view of these structures in the $\langle 100 \rangle$ -oriented foils, since the different colonies overlap. A better chance of evidence is provided by $\langle 111 \rangle$ -oriented foils, as here one set of the colonies has its longitudinal axis perpendicular to the foil surface. Thus, the triangular structures (marked C_1 - C_2 - C_3) of Fig. 6 can be assigned to the threefold colony structure described above. The longitudinal axis is oriented edge-on, and the domains lie on three different $\{110\}$ planes, symmetrically inclined to the $\langle 111 \rangle$ axis and intersecting the surface along $\langle 110 \rangle$ directions. Similar colony structures elongated along the inclined $\langle 111 \rangle$ directions are hardly recognizable, owing to the contrasting superposition. In addition to these symmetric colony arrangements, competing structures of growth appear as, e.g., those with domains greatly enlarged in one lateral dimension.

The lateral extension of the domains during the ferroic transition,¹² from the cubic to the metastable tetragonal phase probably does not occur as an instantaneous single-step process.

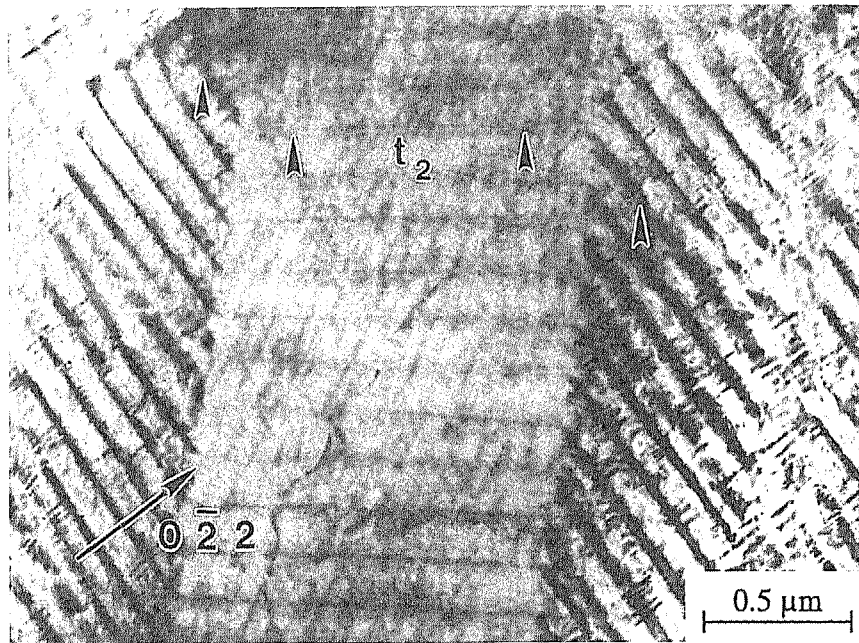


Fig. 3. Colonies under imaging conditions in which the extension of one domain variant across the colony boundary is visible. Close to the $[100]$ pole.

Numerous fine antiphase boundaries inside the domains (Fig. 7) as well as observations in partially stabilized tetragonal zirconia¹³ indicate that these domains themselves are originally composed of different tiny domains, which afterwards turn into one particular variant. In Ref. 13, the platelike domains of a colony in the outer region exhibit a substructure, which means that in those regions the plates consist of very small different domain variants themselves. Thus, they exhibit the same structure as the colonies on another scale so that self-similar structures arise.

The colonies and their substructures obviously represent an optimum accommodation of the spontaneous strain caused by the ferroic phase transition from the cubic to the tetragonal phase. In the following, this strain and its consequences will be treated in more detail. During the cubic-to-tetragonal phase transition, the c -axis of the unit cell is slightly dilated. In t' -ZrO₂ with a Y₂O₃ content of 3 mol%, the dilation amounts to less than 1%, which is about half the value of pure ZrO₂ with a

c/a ratio of 1.02.¹⁴ This dilatation, also called tetragonality, determines the mutual orientation of the c -axes of twinned domains. It is well established that inside the colonies the domains share coherent low-energy $\{110\}$ twin planes. Consequently, their c -axes are not orthogonal to each other, however, making an angle of 89.4° for 1% tetragonality. Figure 8(a) schematically shows the relation between domain variants t_2 and t_3 inside a colony C_3 (cf. Fig. 2(b)). The c -axes of the

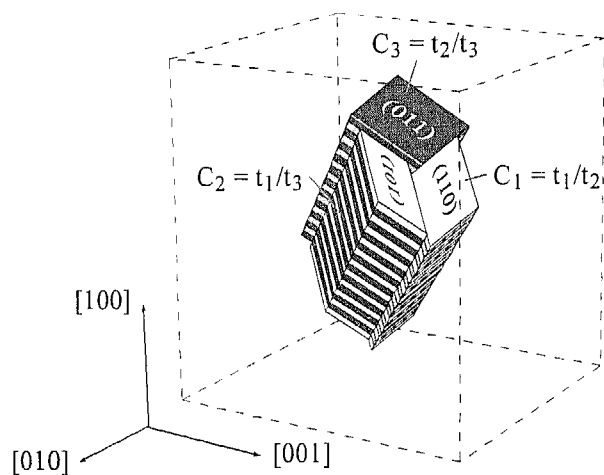


Fig. 4. Three-dimensional shape of the colonies created of tetragonal domains, differently arranged with respect to the $\langle 111 \rangle$ longitudinal colony axis. At the $(0\bar{1}1)$ colony boundary between C_1 and C_2 , the domain t_1 is common to both colonies and t_2 adjoins t_1 ; at $(10\bar{1})$ between C_1 and C_3 , t_2 is common and t_1 adjoins t_3 , and at $(\bar{1}10)$ between C_2 and C_3 , t_3 is common and t_1 adjoins t_2 .

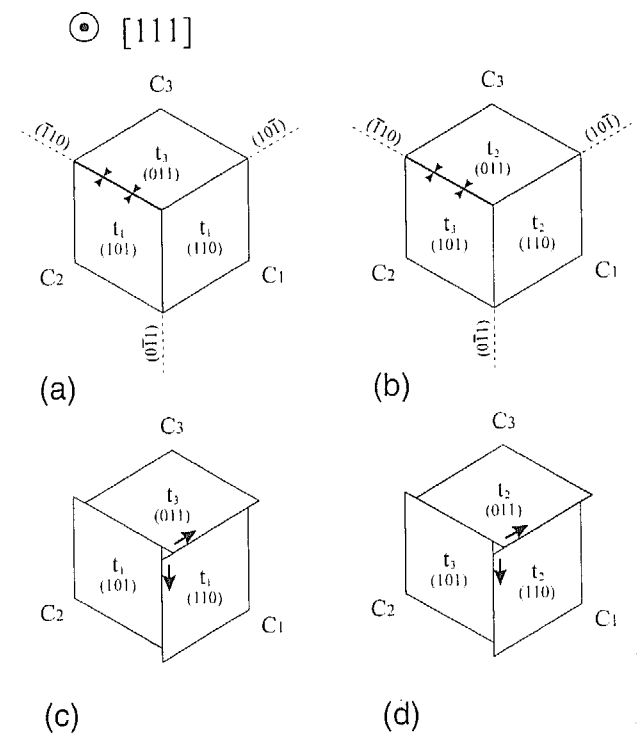


Fig. 5. Schematic view in $[111]$ projection on two layers of an arrangement of three colonies. (a) and (b) show successive layers with the domains exactly meeting at the center, (c) and (d) show a helical arrangement.

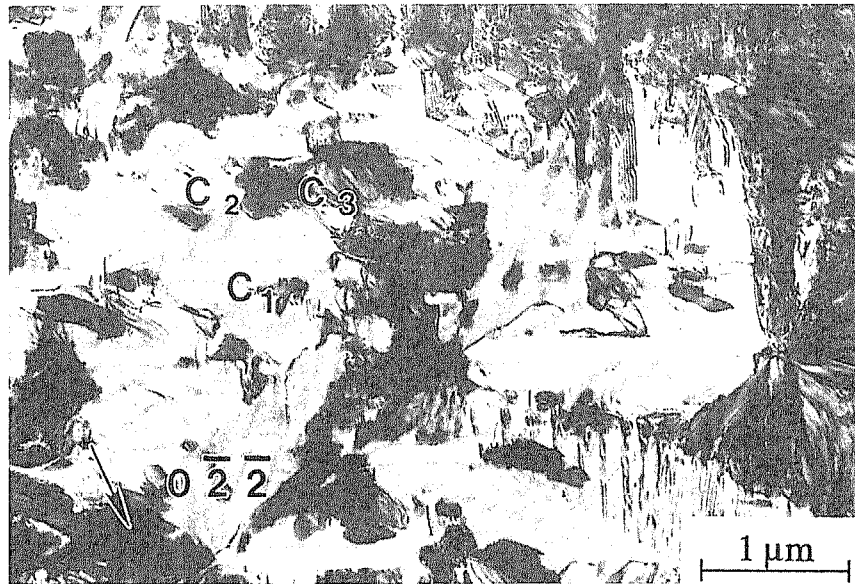


Fig. 6. Tetragonal domains forming colonies in a (111)-oriented TEM foil. C_1 – C_2 – C_3 mark the screw-shaped colony structures of Fig. 4, which are oriented edge-on.

different domains are marked by arrows. Contrary to the situation inside a colony, at a colony boundary the contiguous domains deviate slightly from their ideal twin orientation. Let us consider two colonies C_1 and C_2 of Fig. 2(b), which are composed of alternating domains t_1/t_2 and t_1/t_3 , and which adjoin along a $(01\bar{1})$ plane. Hence, at the colony boundary, t_2 meets t_3 , and t_1 exists in both colonies. This configuration is schematically drawn in Figs. 8(b) and (c). All c -axes are again marked by arrows, and the c -axis of variant t_1 as well as the colony boundary is arranged perpendicularly to the drawing plane. In Fig. 8(b) it is assumed that there is no orientation difference between domains t_1 , which belong to different colonies. Besides, it is obvious that an undisturbed lattice structure in one domain pair t_1 results in a considerable misfit of the adjacent domains at the colony boundary. These disturbances can be reduced at the expense of a slight misorientation between domains t_1 by tilting both colonies around a $[\bar{1}11]$ axis. The result is outlined in Fig. 8(c), where both the domains t_1 deviate

from their common orientation, and t_2/t_3 from their twin orientation. At the colony boundary, regions of lattice dilatation alternate with those of compression.

We propose that an equilibrium state will be achieved in which domains t_1 differ slightly from their common orientation, while t_2 and t_3 approach the twin orientation, resulting in a slight tilt of about 0.5° of both the colonies towards each other. This tilt is difficult to measure directly even if high-resolution electron microscopy is applied. However, specific satellite spots appear in the diffraction patterns. The situation of viewing along a $[100]$ zone axis with the domain boundaries edge-on is described in Ref. 15. For domains with boundaries inclined to the image plane, the twinned lattice only slightly changes the excitation conditions; this effect is negligible under HVEM conditions. But at these domains the inclined domain boundaries should cause a degeneration of the reciprocal lattice points into spikes perpendicular to the domain boundaries, i.e., at an angle of 45° to the image plane. Owing to this degeneracy,

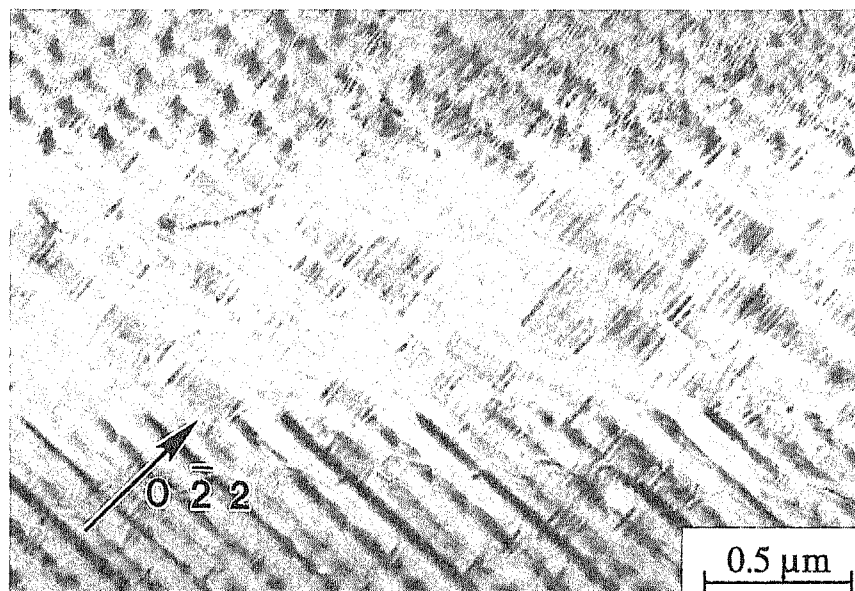


Fig. 7. Small antiphase domain boundaries inside the domains of a colony imaged by fringe contrast. Close to the $[100]$ pole.

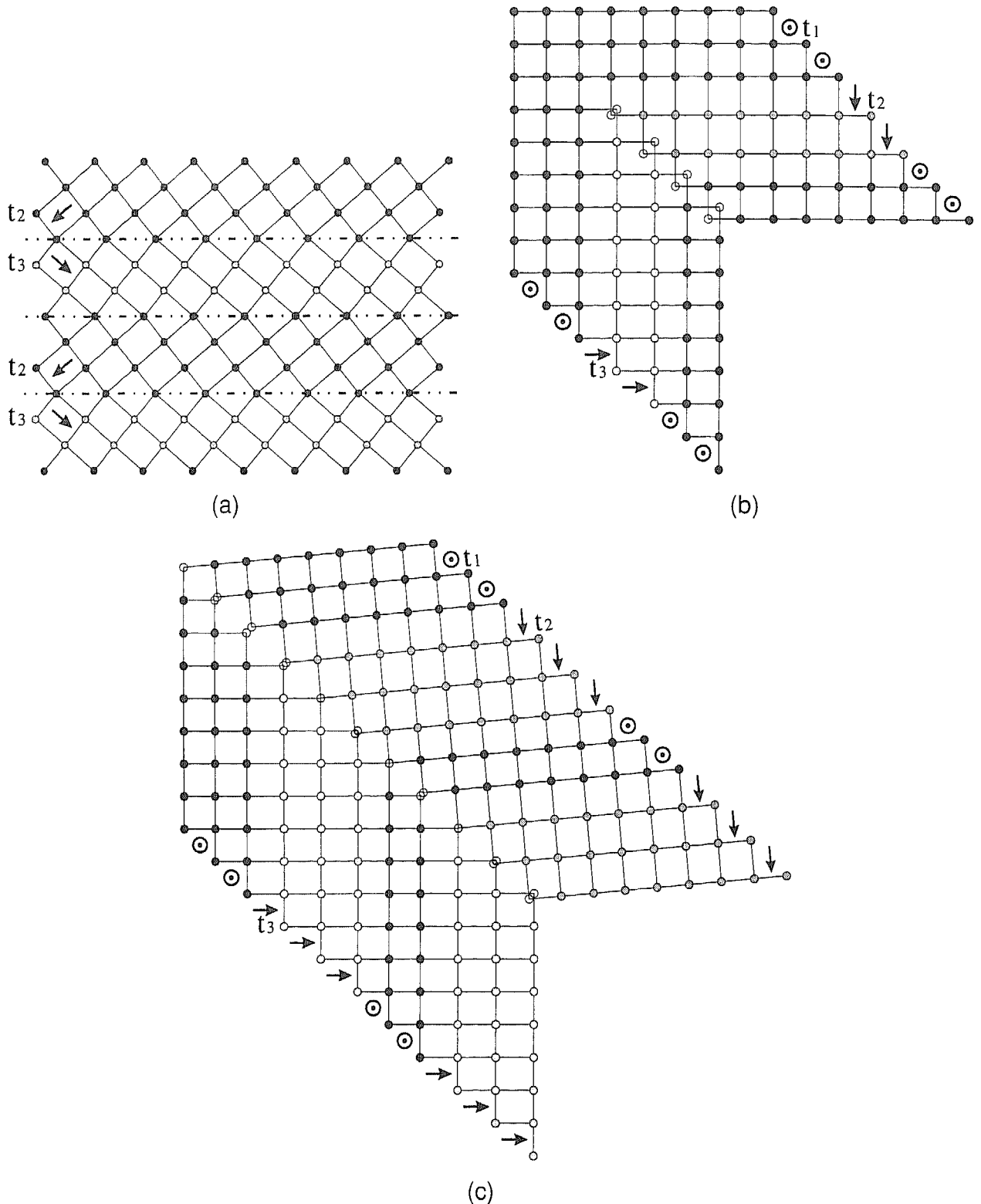


Fig. 8. Schematic drawing of the structure of twinned domains. The c -axes of the different domains are marked by arrows. The open circles indicate the atomic positions of the undisturbed lattice. (a) Domain variants t_2 and t_3 inside a colony C_3 (cf. Fig. 2(b)). The domain boundaries are perpendicular to the drawing plane. (b) Domains t_1/t_2 in colony C_1 , and t_1/t_3 in C_2 adjoin along a $(01\bar{1})$ plane (cf. Fig. 2(a)); common orientation of domain variants t_1 . (c) Structure of (b) after a slight mutual tilt of the colonies.

satellite spots arise, especially for the high-order reflections. However, these satellites are shifted in $\langle 001 \rangle$ directions perpendicular to the intersection line of the twin boundaries with the image plane (cf. Fig. 2(a)). Figure 9(a) shows colonies composed exclusively of domains with inclined boundaries. The intersection lines between the domain boundaries and the

image plane run in horizontal and vertical directions in accordance with the $\langle 100 \rangle$ directions of the corresponding diffraction pattern. In the case of these inclined domain boundaries, only satellites shifted in $\langle 100 \rangle$ directions are expected. Nevertheless, the diffraction spots in Fig. 9(b) are split also in the $[01\bar{1}]$ direction perpendicular to the colony boundary (marked by

arrows), indicating a mutual tilt of about 0.5° between the colonies as a whole, in accordance with the theoretical considerations above.

Besides the very regular colony structures mentioned above, there are often colonies in more or less random arrangement. For instance, Fig. 10 shows a region where colonies extending in different $\langle 111 \rangle$ directions join each other. A rather exceptional case is demonstrated in Fig. 11. In the position marked by arrows, the domains of the colony with the stacking sequence t_1/t_2 perpendicularly meet one domain t_1 of a second colony. While domains t_1 of both colonies extend directly into each other, domains t_2 are separated from t_1 of the second colony by domain walls. A closer inspection of the interface region reveals a change in the domain thickness. Here, a well-known equilibrium configuration is formed¹² by the t_2 domains broadening at the expense of t_1 .

IV. Conclusions

(a) HVEM enabled the analysis of the microstructure of tetragonal polydomain zirconia in relatively thick foils. The different structures observed in transmission electron micrographs can be derived from a single morphology of colonies of tetragonal domains. In this morphology, the colonies are

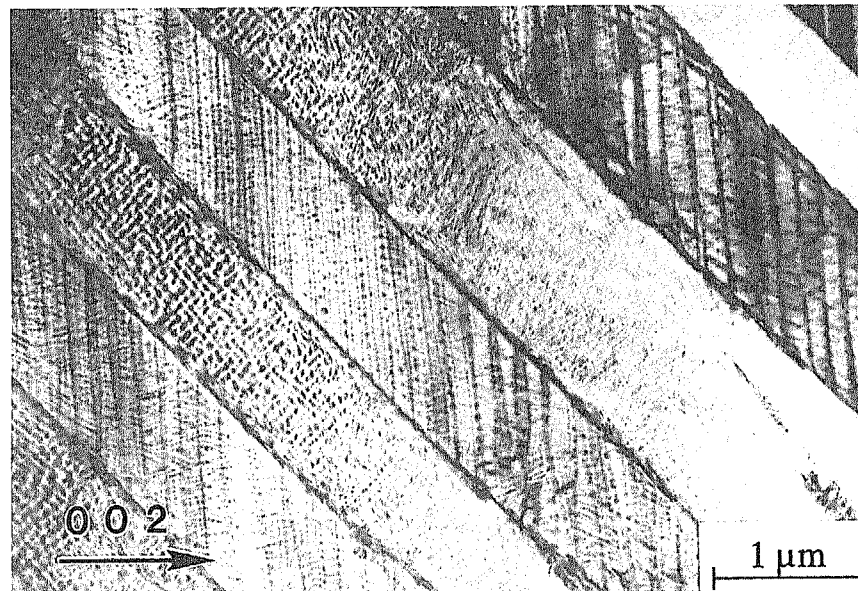
extended in $\langle 111 \rangle$ directions. They either form an accordionlike structure by a repeated stacking of two types of colonies, or three colonies always join along their longitudinal axis in a helical arrangement of the individual domains.

(b) Like the domain boundaries, the colony boundaries are $\{110\}$ planes. In every second layer, one domain variant extends across the colony boundary. In the remaining layers, the colony boundary is a twin plane of the adjoining domains. In this way, the colony boundaries are smooth, in contrast to the boundaries between the colonies and the matrix in partially stabilized zirconia.

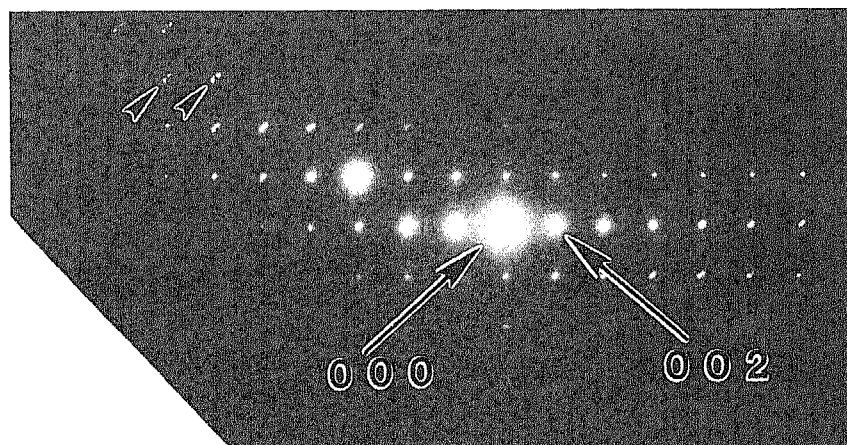
(c) The specific morphology represents a highly ordered structure, which obviously efficiently relaxes the strains after ferroelastic transformation.

(d) In structures less regular than the accordionlike structures or the structures of three-fold symmetry, the domains as well as the colonies are still always bound by $\{110\}$ planes, which act as twin planes for other adjoining domains or colonies.

(e) This twin-related arrangement and the extensive relaxation of the ferroelastic strains by the alternate stacking of different domains and colonies are the basis of the coherence of large macroscopic polydomain crystals.



(a)



(b)

Fig. 9. Colonies consisting exclusively of inclined domains causing a splitting of diffraction spots in the $[01\bar{1}]$ direction perpendicular to the colony boundary. Close to the $[100]$ pole. (a) TEM micrograph, (b) diffraction pattern.

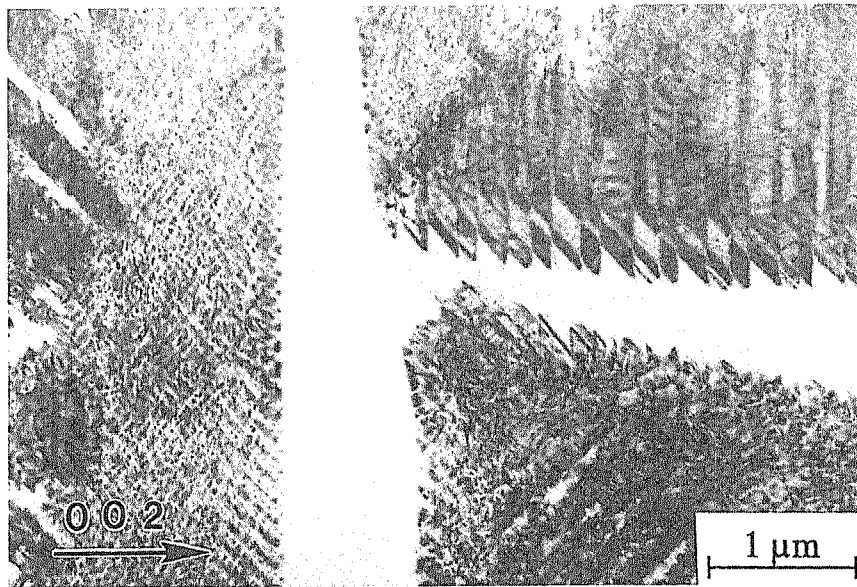


Fig. 10. Adjoining colonies of tetragonal domains with different longitudinal axes along $\langle 111 \rangle$. Close to the $[100]$ pole.

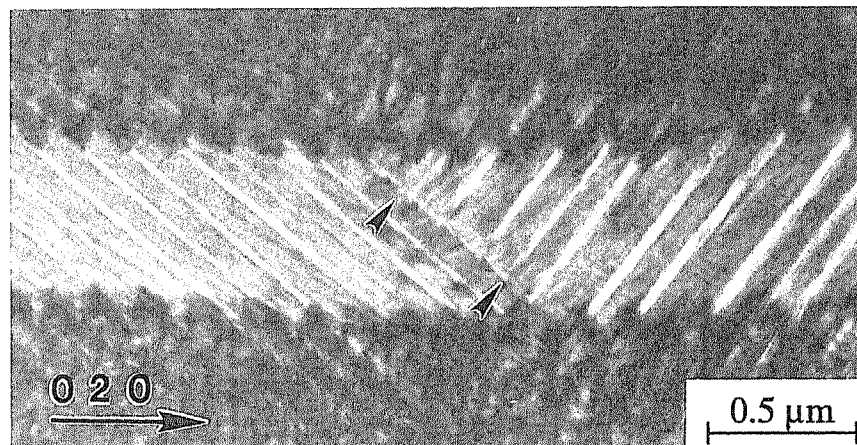


Fig. 11. Domains of two colonies perpendicularly contiguous to each other (marked by arrows). Close to the $[100]$ pole.

Acknowledgments: The authors thank the staff of the Halle HVEM for keeping the instrument in good condition and for permanent help.

References

- ¹C.-J. Chan, F. F. Lange, M. Rühle, J. F. Jue, and A. V. Virkar, "Ferroelastic Domain Switching in Tetragonal Zirconia Single Crystals—Microstructural Aspects," *J. Am. Ceram. Soc.*, **74**, 807–13 (1991).
- ²R. P. Ingel, D. Lewis, B. A. Bender, and R. W. Rice, "Physical, Microstructural, and Thermomechanical Properties of ZrO_2 Single Crystals"; pp. 408–14 in *Advances in Ceramics*, Vol. 12, *Science and Technology of Zirconia II*, Edited by N. Claussen, M. Rühle, and A. Heuer. American Ceramic Society, Columbus, OH, 1984.
- ³K. M. Prettyman, J.-F. Jue, A. V. Virkar, C. R. Hubbard, O. B. Cavin, and M. K. Ferber, "Hysteresis Effects in 3 mol% Ytria-Doped Zirconia (t' -Phase)," *J. Mater. Sci.*, **27**, 4167–74 (1992).
- ⁴V. K. Wadhawan, "Ferroelasticity and Related Properties of Crystals"; pp. 3–103, in *Phase Transitions*, Vol. 3, Gordon and Breach Science Publishers, New York, 1982.
- ⁵A. V. Virkar and R. L. K. Matsumoto, "Toughening Mechanism in Tetragonal Zirconia Polycrystalline (TZP) Ceramics"; pp. 653–63 in *Advances in Ceramics*, Vol. 24, *Science and Technology of Zirconia III*, Edited by S. Somiya, N. Yamamoto, and H. Yanagida. American Ceramic Society, Westerville, OH, 1988.
- ⁶J. F. Jue and A. V. Virkar, "Fabrication, Microstructural Characterization, and Mechanical Properties of Polycrystalline t' -Zirconia," *J. Am. Ceram. Soc.*, **73**, 3650–57 (1990).

⁷C. J. Chan, F. F. Lange, M. Rühle, J.-F. Jue, and A. V. Virkar, "Ferroelastic Domain Switching in Tetragonal Zirconia," *Mater. Res. Soc. Symp. Proc.*, **209**, 725–30 (1990).

⁸A. Foitzik, M. Stadtwald-Klenke, and M. Rühle, "Ferroelasticity of t' - ZrO_2 ," *Z. Metallkd.*, **84**, 397–404 (1995).

⁹M. Stadtwald-Klenke, "Elektronenmikroskopische Untersuchungen an Inneren Grenzflächen in Verschiedenen mit Y_2O_3 Dotierten ZrO_2 -Keramiken"; Ph.D. Dissertation, Stuttgart University, 1994.

¹⁰D. Baither, B. Baufeld, and U. Messerschmidt, "Morphology of Tetragonal Precipitates in Y_2O_3 -Stabilized ZrO_2 Crystals," *Phys. Status Solidi (a)*, **137**, 569–76 (1993).

¹¹A. H. Heuer, V. Lanteri, and A. Dominguez-Rodriguez, "High Temperature Precipitation Hardening of Y_2O_3 Partially-Stabilized ZrO_2 (Y-PSZ) Single Crystals," *Acta Metall.*, **37**, 559–67 (1989).

¹²E. K. H. Salje, "Phase Transitions in Ferroelastic and Coelastic Crystals"; in *Cambridge Topics in Mineral Physics and Chemistry*. Cambridge University Press, Cambridge, U.K., 1990.

¹³B. Baufeld, D. Baither, U. Messerschmidt, and M. Bartsch, "High Voltage Electron Microscopy *in situ* Study on the Plastic Deformation of Partially Stabilized Tetragonal Zirconia," *Phys. Status Solidi (a)*, **150**, 297–306 (1995).

¹⁴A. H. Heuer, R. Chaim, and V. Lanteri, "Review: Phase Transformations and Microstructural Characterization of Alloys in the System Y_2O_3 - ZrO_2 "; see Ref. 5, pp. 3–20.

¹⁵N. Ishizawa, A. Saiki, T. Yagi, N. Mizutani, and M. Kato, "Twin-Related Tetragonal Variants in Ytria Partially Stabilized Zirconia," *J. Am. Ceram. Soc.*, **69**, C-18–C-20 (1986). □